

Flat slabs with spherical voids. Part II: Experimental tests concerning shear strength

Mihai Bindea^{*1}, Raul Zagon², Zoltan Kiss³

^{1,2,3} *Technical University of Cluj-Napoca, Faculty of Civil Engineering, 15 C Daicoviciu Str., 400020, Cluj-Napoca, Romania*

Received 26 February 2013; Accepted 15 August 2013

Abstract

The behavior of spherical hollow core flat slabs subjected to shear strength is an issue of great importance for the sizing and designing phase of this type of floor systems. This paper presents two series of experimental tests regarding the shear load-carrying capacity of spherical hollow flat slabs in case of low levels of longitudinal reinforcement. The test results point to a low rate of shear failure in the case of hollow flat slabs with reinforcement percentages below 0.5%, whereas in case of reinforcement percentages close to 0.5%, the ultimate shear force is almost equal to the maximum value of the solid slab with the same bending capacity but lower height.

Rezumat

Comportarea planșelor dală cu goluri sferice la forță tăietoare este un aspect foarte important în faza de calcul și de proiectare a acestor tipuri de planșee. Lucrarea de față prezintă două serii de teste experimentale cu privire la capacitatea portantă la forță tăietoare a planșeelor dală cu goluri sferice în cazul unor procente mici de armare longitudinală. Rezultatele indică un risc scăzut de cedare la forță tăietoare pentru dalele cu goluri cu procente de armare sub 0.5%, iar în cazul dalei cu goluri cu procentul de armare de 0.52% forța tăietoare ultimă este foarte apropiată de valoarea maximă aferentă dalei pline de aceeași capacitate portantă la încovoiere, dar cu înălțime mai mică.

Keywords: shear failure, flexural failure, concrete slab, flat plate, spherical hollow cores

1. Introduction

Among all type of slabs used on multi-storey buildings, the flat slabs present the most advantages from technical to functional point of view. There are different technical solutions to design a hollow flat slab. One of the most popular method is to replace the concrete from the median zone of the slab with plastic spheres. Comparatively to using normal flat slabs, this method can entail reduced quantities of concrete, particularly for large openings. In addition to concrete quantity reduction, within certain limits of application, this constructive solution provides the same biaxial bending capacity of slabs as the normal ones.

The removal of the unused concrete from the tensile zone of the cross section results in a decrease of the shear load-carrying capacity. Even if the hollows are eliminated from the action area of the shear punching stresses around the columns, in order to determine the perimeter of the full slab with

* Corresponding author: Tel./ Fax.: 0040 264 401545
E-mail address: mihai.bindea@dst.utcluj.ro

a high extent of accuracy, it must be known the maximum shear force which the spherical hollow flat slabs can sustain.

According to EC2 [1] and ModelCode2010 [2], the minimum width of the transversal section, b_w interferes in the calculation formula for shear bearing capacity. Because in hollow flat slabs with plastic spheres it is 10% from a normal flat slab, the specific literature advances other alternative methods for the design of shear capacity.

Such alternative methods propose a ratio of reduction (around and over the value of 0.6 [3][4]) to the load-bearing capacity determined for the full slab. The reduction ratio was determined from repeated experimental tests on hollow flat slabs with longitudinal reinforcement percentages higher than 0.50%. Nevertheless, there are many situations when the hollow flat slab supported on columns or/and bearing walls has the longitudinal reinforcement percentages lower than 0.50%. This could be in the cases with small to medium loads (characteristic value for the variable load under 5kN/m^2) and not to large openings (under 10m).

2. Experimental program

The experimental program focused on studying the behavior of hollow flat slabs with spherical void formers at shear force. The experimental tests were performed in the Laboratory of Civil Engineering Faculty of Cluj Napoca. Four hollow flat slabs and one normal flat slab were made. The steel lattice unit and the plastic balls were provided by the company Bubbledeck Romania. The proposed reinforcement is shown in Table 1.

Table 1: Elements dimensions and reinforcement percentages

Name	Series	B x L x H [mm]	d [mm]	Longitudinal reinforcement	A_{sl} [cm ²]	ρ_{sl}
DG1	I	1500x2750x310	250	12Ø8+2Ø6	6.60 cm ²	0.18%
DG2		1500x2750x310	250	12Ø8+2Ø6	6.60 cm ²	0.18%
DG3	II	1500x2850x310	250	12Ø8+2Ø6+12Ø12	20.16 cm ²	0.52%
DG4		1500x2850x310	250	12Ø8+2Ø6+7Ø10	12.10 cm ²	0.31%
DP1		1500x2850x250	230	10Ø10+12Ø12	21.41 cm ²	0.63%

The welded mesh reinforcement was made of PC52 steel type with Ø8mm bars for the bottom side and Ø6mm bars for the top side of the elements. The longitudinal inclined reinforcement was made from welded Ø6mm bars with flat profile. The concrete used in this experiment was C20/25, ordered from a local concrete plant. To establish the compressive strength, six samples were taken on 150mm cubes. The compression tests were performed, according to [5], at intervals of 28 days and on the day of the tests, by means of the testing device of UTC-N Central Laboratory - Advantest 9. The average compressive strength of the concrete cubes was $f_{cm_cube}=30.4\text{MPa}$ at 28 days, and $f_{cm_cube}=50.3\text{MPa}$.

2.1 Test set-up

The tests were made on four point bending. As shown in Fig. 1, the test bench was made of steel profiles with H section connected with bolts. The elements were loaded until breaking in a single phase.

The force increased with every loading step by a 10kN increment. There have been recorded data related to: force intensity, three point vertical deflections in the middle of the slab, vertical deflections in the four corners of the slab, specific deformations on the lateral sides of the element

and the opening and length of the cracks.

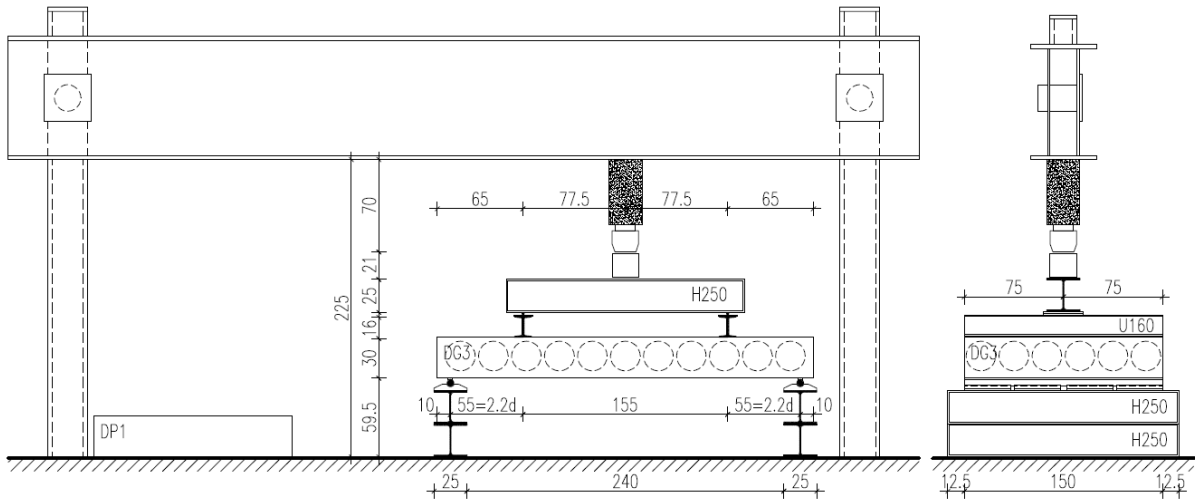


Figure 1. Test bench

2.2. Test elements from series one

The DG1 and DG2 elements had a similar configuration, except for the a/d ratio ($a/d=2.4$ for DG1 and $a/d=1.8$ for DG2). The minimum longitudinal reinforcement percentage was used, according to EC2. For DG1 the first perpendicular cracks were observed in the median zone on both lateral sides of the slab. The value of force at this point was $F_{cr1}=120\text{kN}$. Further on, the cracks extended to the length of the element but no farther than the force position (Fig. 2). No inclined shear cracks were observed. Length and opening of the cracks were monitored until the opening for a crack reached values equal to 0.5mm , corresponding to $F'_{cr1}=180\text{kN}$.

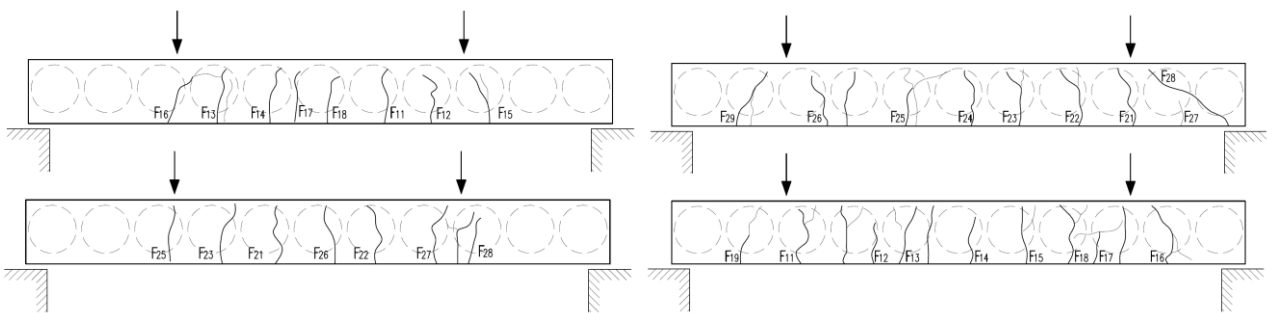


Figure 2. Cracks for DG1 (left) and DG2 (right)

For DG2 slab, the force which caused the first crack was $F_{cr2}=240\text{kN}$. Along with increasing the load, it can be noticed that the cracks exceeded, as opposed to DG1, the load position. Moreover, shear cracks appeared for a force equal to $F'_{cr2}=460\text{kN}$.

If the spheres and cracks position are overlapped, it can be observed, as shown in the figure 2, that for both slabs, the cracks' position coincides with that of the spheres. Furthermore, most of the cracks were positioned in the central area, between force positions.

Figure 3 presents the force-deflection relationship recorded for DG1 and DG1 slabs. In Figure 3 it can be observed the failure, for both elements, that was produced by the yielding of the reinforcement at the same time with excessive deflections. This behavior resulted in big openings for cracks, more than the limit imposed by service load criteria. The test was discontinued when a deflection equal to $L/50=51\text{mm}$ was observed. The force recorded for this deflection was $F_u=240\text{kN}$

with first slab, respectively $F_u=460\text{kN}$ with the second one.

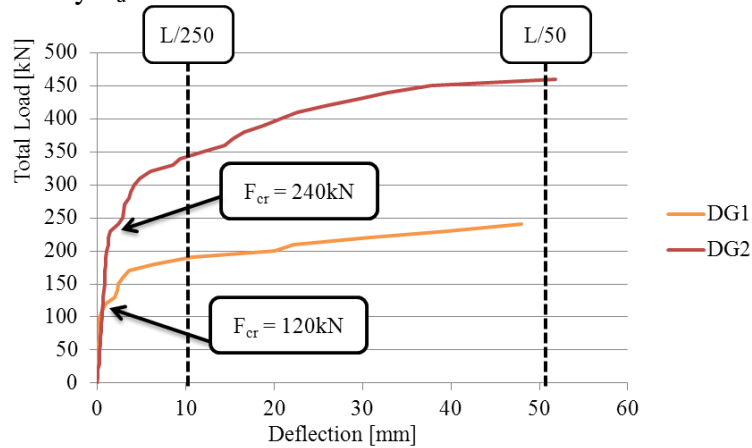


Figure 3. Force-deflection diagrams – elements DG1 and DG2

2.3. Test elements from series two

The a/d ratio varied for the slabs in this series as well. The DG3 and DG4 slabs had the same geometrical characteristics and mechanical properties for concrete. The DP1 plate was tested in the same conditions as the DG3 slab. The difference between the slabs came from the percentage of reinforcement used. The main parameters observed were the vertical deflection relative to applied load, the development of cracks along the lateral sides of the element and the strains in the transversal direction of the slab.

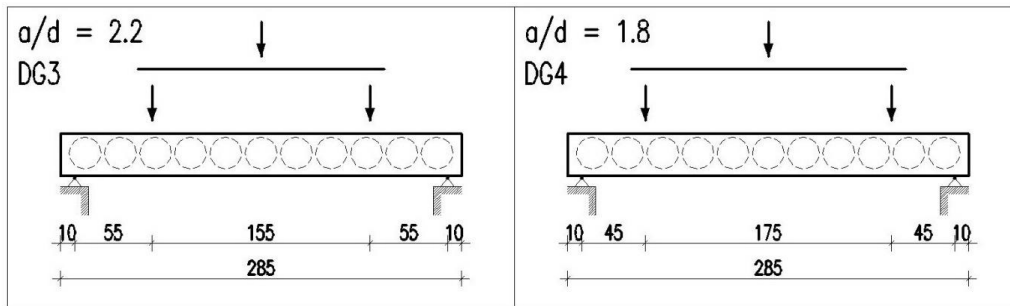


Figure 4. Test set-up for DG3 (same for DP1) and DG4

2.3.1 Results for slab DG3

The first cracks, perpendicular to the longitudinal axis of the element (Fig. 5), were noticed for a load of $F_{cr1}=160\text{kN}$.

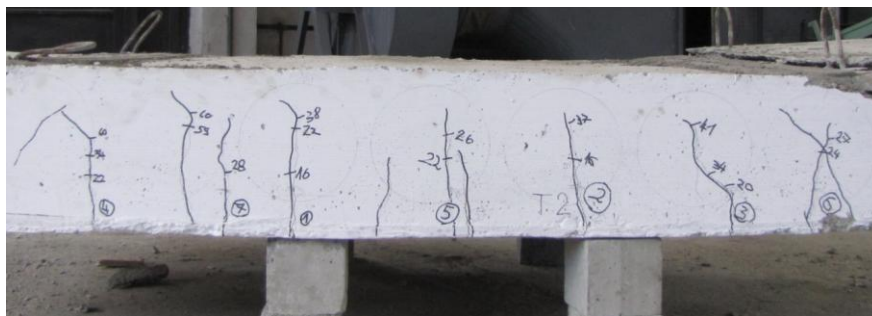


Figure 5. The central cracks positions on the longitudinal face – element DG3

The first inclined cracks appeared between supports and the load lines for a total force of 363.6kN (F_{cr2}). The opening for inclined cracks was evaluated until the recorded value reached $w=0.3mm$, for a total load $F'_{cr2}=460kN$. For this force the perpendicular cracks had the opening around 0.20mm. After the inclined cracks were observed, closely to the ultimate load value, it can be noticed vertical and horizontal cracks on the short lateral side of the element (Fig. 6). This behavior can be explained by the occurrence of the transversal tensile stresses, which appears due to the blocking effect of spherical voids in the flowing direction of the compressive stresses trough the concrete strut. The horizontal cracks appeared in the slab median zone intersecting the smallest concrete sections which connect the bottom and top side of the slab.



Figure 6. The cracks positions on the lateral and transversal side of the element DG3

Breaking came suddenly by stroking the compressive concrete through crack F9 at a maximum load of 756kN (Fig.7). The maximum deflection, recorded at breaking point, was about 31.3mm (Fig. 8).



Figure 7. Breaking moment – element DG3

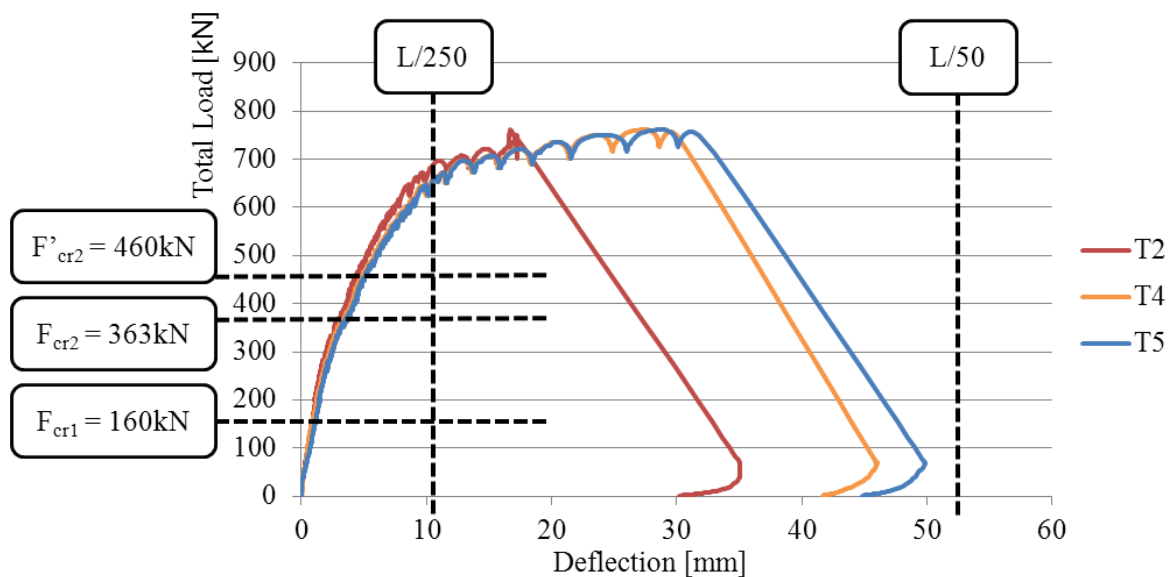


Figure 8. Force – deflection diagram for element DG3

2.3.3 Results for slab DG4

The first cracks were found in the median area of the element, for a force $F_{cr1}=182kN$. With the increasing of the force, the cracks extended over the entire area between the force positions. There also appeared cracks in the area between the forces and the supports, in close proximity of the forces positions. The opening and lengths of the cracks were measured until the value reached $w=0.3mm$, at an intensity of $F_{cr2}=335kN$. Figure 9 illustrates the crack configuration on the longitudinal face of the element. In this case there were no cracks on the short lateral side of the element.

It can be noted that towards the edges of the slab, in the vicinity of the stands, the normal cracks developed towards the compressive area, tilted against the axis on the length of the element. The explanation underlying this phenomenon resides in the fact that the concrete blocks between the cracks were subjected to bending as simple cantilevers and the reinforced slab transforms into a comb-like structure. Also, it can be seen from figure 9 that the cracks appeared in front of the transversal voids lines.

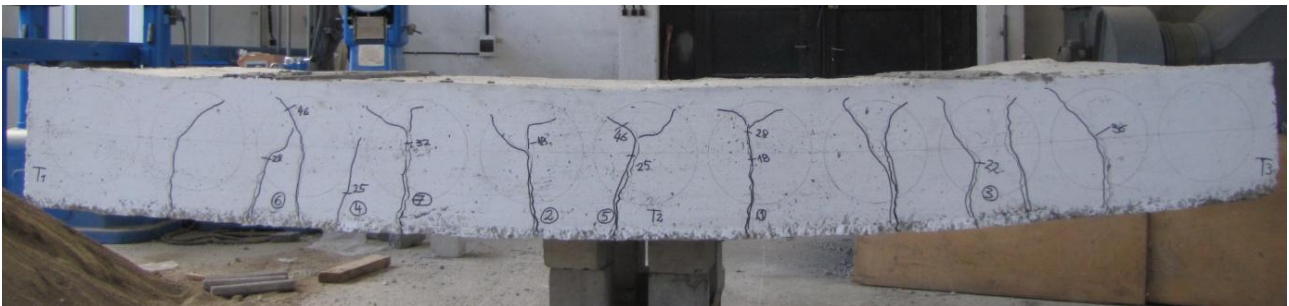


Figure 9. Cracks review on lateral side – DG4 slab

The DG4 slab failed under the bending moment. The test was stopped after the longitudinal reinforcements had exceeded the yield strength and the vertical deflection increased the limit value of $L/50=53mm$. The maximum deflection located in the middle of the slab measured 61.7mm. Figure 10 illustrates the force – deflection diagram for DG4.

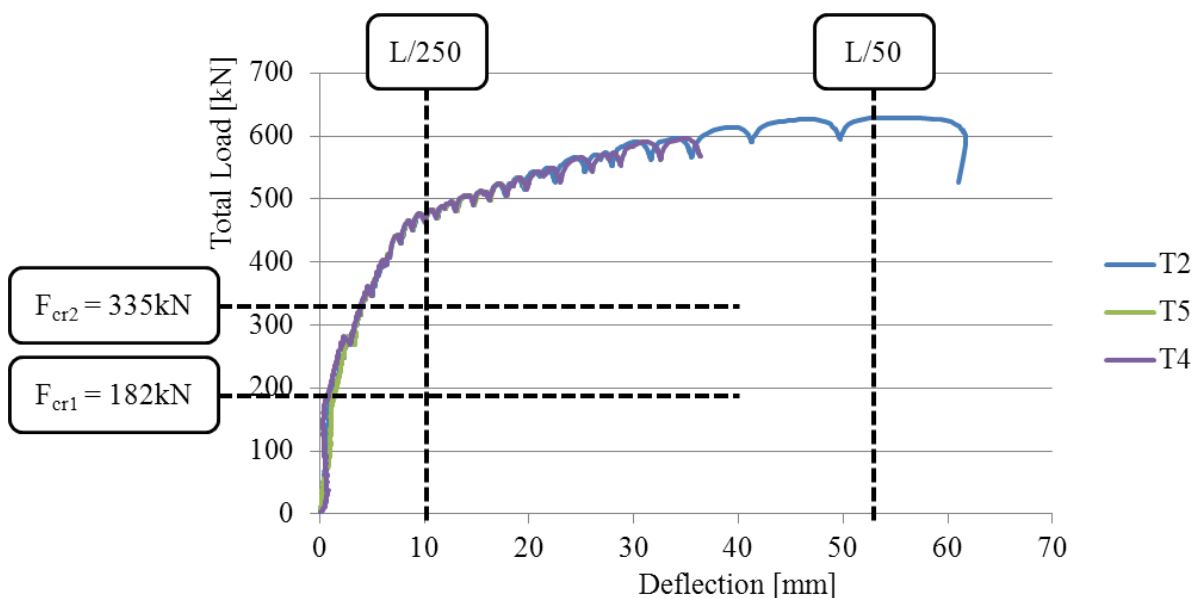


Figure 10. Force – deflection diagram for element DG4

2.3.4 Results for slab DP1

At the maximum force of 680kN and a corresponding vertical deflection of 25mm , the test came to an end due to technical problems which had occurred before the slab could be considered failed. The first vertical cracks appeared in the central area of the element, at a force value of $F_{cr}=202\text{kN}$. The cracks escalated across the entire length of the slab, and towards the stands they went beyond the force positions. The cracks between the stands and the forces evolved to the compression zone in the upper end, inclined against the slab longitudinal axis (Fig. 11), yet less obvious as compared to the DG4 slab. Figure 11 presents the crack survey, and it can be noticed the orderly arrangement of the cracks, at a shorter distance than in the case of hollow slabs, where cracks tended to develop mostly in front of the hollows.

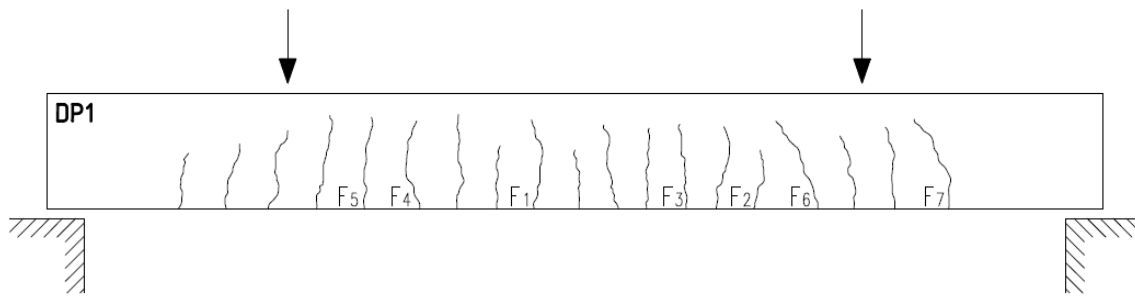


Figure 11. Cracks review on lateral side – DP1 slab

Since the tested element has not exhausted its bending strength, the experiment was resumed later, and the only measurements that have been carried out were in relation to the value of the force and the three-point vertical deflections in the central part of the slab. The second loading cycle was stopped after the boundary limit of $L/50$ for the maximum deflection was exceeded. The slab failed due to bending moment, developing excessive deflections, along with the increase in the cracks openings. No inclined cracks developed in the shear force action area. The curves for the two loading cycles and the curve corresponding to DG3 element, are presented in Figure 12 below.

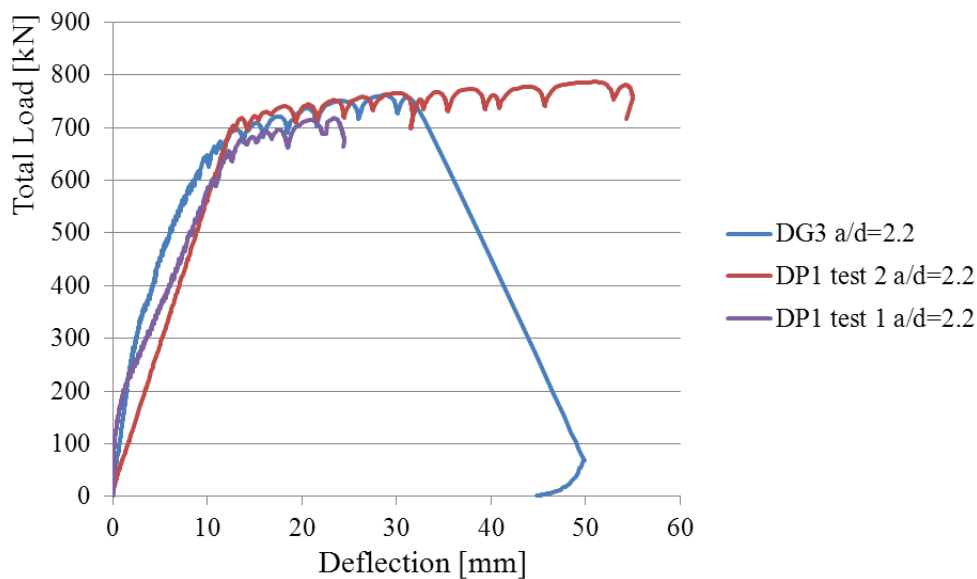


Figure 12. Force – deflection diagram – element DP1 and DG3

3. Conclusions

For element DG3, it has been recorded the value of the shear force upon occurrence of the first inclined cracks ($V_{Ed,cr}$), and the maximum value of shear force ($V_{Ed,u}$) corresponding to the breaking point in shear failure.

In the cases of the elements DG2 and DG4 that did not develop inclined cracks, $V_{Ed,cr}$ has been considered the shear force which caused the extension of the normal cracks, located between the supports and the force positions, towards the concrete compression zone, tilted against the axis of the slab. Also for these elements considering the flexural failure mode the ultimate shear force was recorded at the moment when the vertical displacements reached the limit value $L/50$.

The DG1 slab produced no cracks in the area between the stands and the loadings, and for the DP1 slab the inclined cracks near the supports were less obvious. As regards the DG2 and DG4 slabs, since $a_v < 2d$, it is considered that a part of the loading force $\Delta P = P \cdot \left(1 - \frac{a_v}{2 \cdot d}\right)$ is directly transferred upon the supports, through the compressed strut [6].

Table 2: Results – shear force

slab	a/d	$V_{Rdc,DP}$ [kN]	$V_{Ed,cr}$ [kN]	$V_{Ed,u}$ [kN]	$V_{Ed,cr} / V_{Rdc,DP}$	$V_{Ed,u} / V_{Rdc,DP}$
DG1	2.4	134.92	-	123	-	0.91
DG2	1.8	134.92	120	196.5	0.89	1.46
DG3	2.2	241.06	184.8	381	0.77	1.58
DG4	1.8	203.52	165	285.6	0.81	1.40
DP1	2.2	237.52	-	393	-	1.65

Since it had the greatest reinforcement percentage ($p=0.52\%$), the DG3 slab failed due to shear force through inclined cracks. The first inclined crack appeared at the shear force which represents 77% of the shear strength calculated according to [1] for a reinforced concrete solid slab of the same width, $V_{Rdc,DP}$, and the inclined cracks opening measured 0.3mm (the limit according to service limit state [1]) at the shear force value which represents 97% of $V_{Rdc,DP}$. The shear force corresponding to the SLS limit through the crack width criteria was below the shear force corresponding to the yielding moment for reinforcement. The ultimate shear force of element DG3 is very similar with the maximum shear force applied on the DP1 slab, $V_{Ed,u,DG3} = 97\% V_{Ed,u,DP1}$. Taking into consideration that the results obtained for the two elements were also similar with regard to the bending moment, it can be concluded that in relation to the shear load carrying capacity for low percentage reinforcement slabs, the influence of spherical hollow cores is far less important than implied in the specific literature.

4. References

- [1] SR EN 1992-1-1 2006, *Eurocode 2: Proiectarea structurilor de beton, Partea 1-1: Reguli generale și reguli pentru clădiri*.
- [2] Fib Special Activity Group 5, *Model Code 2010 First Complete Draft*, march 2010.
- [3] BubbleDeck UK Head Office, *BubbleDeck Voided Flat Slab Solution – Technical Manual and Documents*, June 2006.
- [4] Schnellenbach-Held M., Aldejohann M., *Zweiachsige Hohlkorperdecken in Theorie und Versuchen*, BFT Betonwerk + Fertigteil-Technik, 10/2005, pp.50-59.
- [5] RILEM, *RILEM Technical Recommendations for the Testing and Use of Construction Materials*, E&FN Spon, St Edmundsbury Press, Great Britain: International Union of Testing and Use of Construction Materials, 1994.
- [6] Kiss Z., Oneț T., *Proiectarea structurilor de beton după SR EN 1992-1*, Editura Abel 2008.